

Application of linear model of sorption dynamics to the comparison of solid phase extraction systems of phenol

G.I. Tsysin*, I.A. Kovalev, P.N. Nesterenko, N.A. Penner, O.A. Filippov

Department of Chemistry, Moscow State University, Moscow 119899, Russia

Received 23 March 2002; received in revised form 28 September 2002; accepted 1 October 2002

Abstract

A method based on the linear model of sorption dynamics (LMSD) is applied for the comparison of several solid phase extraction systems used for preconcentration of phenol from water solutions. The method includes the calculation of maximum concentration efficiency for the given values of preconcentration factor and recovery under scope of the model. Original parameters of LMSD were obtained from the experimental data on kinetics of sorption of phenol on different hydrophobic non-polar sorbents including poly(styrene-divinylbenzene) (Amberlite XAD-2, PLPR-S 100), hypercrosslinked polystyrene (Purosorb MN-200), hexadecylsilica (KSK-G C₁₆) and others (Amberlite XAD-4, Amberchrom CG-161). The suitability of LMSD for evaluation of dynamic sorption systems is discussed.

© 2002 Elsevier Science B.V. All rights reserved.

Keywords: Solid phase extraction; Phenol; Linear model of sorption dynamics

1. Introduction

Phenol and its derivatives are common reagents in many industrial processes so they are presented in different industrial and wastewaters. Being important water pollutants these compounds have to be under continuous monitoring in different types of water, even at very low concentration level. So, the European Community Directive

specified a legal tolerance level for each phenol to be less than 0.1 $\mu\text{g l}^{-1}$ and to be less than 0.5 $\mu\text{g l}^{-1}$ for the sum of phenols in waters intended for any human consumption. In practice, the phenols are usually determined by reversed phase HPLC with UV [1,2] or electrochemical detection [3]. As it has been noted in many papers, the reliable direct determination of phenols in waters at the concentration level 0.1–0.4 $\mu\text{g l}^{-1}$ is a rather difficult task. So, the preconcentration of phenols from water samples is necessary for their HPLC determination at sub-ppm level [4–11]. Solid phase extraction (SPE) is a common techni-

* Corresponding author.

E-mail address: tsisin@analyt.chem.msu.ru (G.I. Tsysin).

Nomenclature

$a(x, t)$	average concentration of adsorbed substance in bed ($\text{mg (ml of bed)}^{-1}$)
$a^{(s)}(x, t, r)$	local concentration of adsorbed solute inside of sorbent particle ($\text{mg (ml of particle)}^{-1}$)
$a_0 = a(x, \infty, r) = \Gamma c_0$	concentration of adsorbed substance in bed in equilibrium with concentration in mobile phase c_0
β	liquid film coefficient (s^{-1})
$c(x, t)$	concentration of solute in mobile phase (mg ml^{-1})
$c_0 = c(0, t)$	concentration of adsorbed solute at inlet of bed (constant)
D	apparent coefficient of solid diffusion in spherical particles ($\text{cm}^2 \text{s}^{-1}$)
$\varepsilon = V_{\text{pore}}/V_{\text{bed}}$	bed porosity (void volume of bed)
Γ	distribution ratio of adsorbed substance ($\text{ml of liquid phase (ml of bed)}^{-1}$)
$\eta(X, T) = K_{\text{conc}}/\Gamma$	expended capacity of sorbent bed (dimensionless preconcentration factor)
$\chi(X, T) = 1 - R$	cumulative breakthrough (recovery of solute)
K_d	distribution ratio of solute between solid and mobile phases (ml g^{-1})
$K_{\text{conc}} = a/c$	preconcentration factor
k	Langmuir constant (ml g^{-1})
l	height or length of the bed of sorbent (cm)
Q	Langmuir maximum adsorption capacity (mg g^{-1})
$q(X, T) = a(x, t)/a_0$	dimensionless concentration of solute in bed
$q^{(s)}(X, T, \rho) = a^{(s)}(x, t, r)/a_0$	dimensionless concentration of the solute in particle
R	recovery of adsorbed substance
\Re	radius of sorbent particles (cm)
$r(0 \leq r \leq \Re)$	radius-vector in particles (cm)
$\rho = r/\Re$	dimensionless radius-vector in particles
t	time measured from the beginning of solute input (s)
T	dimensionless time
$u(X, T) = c(x, t)/c_0$	dimensionless concentration of adsorbed substance in mobile phase
v	linear flow velocity (cm s^{-1})
w	volume flow rate of liquid (ml s^{-1})
x	distance measured from inlet of bed (cm)
X	dimensionless bed length

que for the preconcentration of phenols, because of its simplicity, possibility to achieve high preconcentration factors in a short time, low risk of sample contamination, and etc. The main problem of SPE of phenols is the low recovery of hydrophilic phenols, in particular of non-substituted phenol. Therefore the development of new and improvement of known types of adsorbents for the preconcentration of phenol remains an important task during almost three decades.

There are three main groups of sorbents used for the preconcentration of phenols. The first one

includes chemically modified silica. The most popular in this group is octadecylsilica or ODS [4,12]. However, chemically modified silica exhibits rather small affinity to phenol and phenol's recovery is low [13]. The second group involves polymeric sorbents, mainly poly(styrene-divinylbenzene)s with different cross-linking degree and porous structure: XAD-2 [13,14], XAD-4 [13,15–18], Bond Elut PPL [10,13], Amberchrom CG-161 [13,19], PLRP-S 100 [13,20]. Recently, a number of new materials based on hypercrosslinked polystyrene and high crosslinked poly(styrene-divinylben-

zene) under trade names LiChrolut EN [8,13,21], Purolite Macronet Hypersol [13,22–25], Isolute ENV [8,13], HYSphere-1 [10,13] and Envi-Chrom P [13,21] appeared. These sorbents have high cross-linking degree (80% and more) and their developed porous structure provides high values of specific surface area. The other feature of these sorbents is increased ability to π – π interactions with aromatic substances. So, the increased recovery of phenol and its hydrophilic derivatives was noticed. The last group of sorbents includes various carbon black modifications such as Carboxpack B [10], carbon fiber [9] and silica coated with porous graphitic carbon or Hypercarb [26] with special high selectivity for polar organics. The main characteristics of these sorbents are summarized in Table 1.

Taking into consideration the big variety of sorbents applied for SPE of phenol and their significantly different properties, it is important to find out suitable criteria for the scientifically justified choice of the most efficient sorbent for dynamic preconcentration of phenol. Usually, such choice is based on the measurement of distribution ratio under static conditions that is not completely correct due to ignoring of considerable role of mass-transfer rate in the recovery of solute under dynamic conditions.

A new approach to the choice of the most efficient dynamic sorption system, based on the linear model of sorption dynamics (LMSD), is proposed in present work and different sorbents are compared for the preconcentration of phenol.

2. Theory

There are two basic models of mass transfer which have been applied to the investigations of phenol sorption: the liquid film diffusion model, considering diffusion of the solute from the solution to the surface of adsorbent as the rate limited factor, and the solid diffusion model, where diffusion of the solute inside sorbent particle is considered as the rate limited factor [27,28]. Brief description of these models is given below.

First of all, there are a number of statements to simplify the consideration of kinetics of sorption in the fixed bed system:

- the adsorbent in a column consists of homogeneous monosize spherical particles;
- the solute containing solution flows through the column/bed with a constant velocity;
- the solution flow is considered both in sorbent bed and in mobile phase volume as in homogeneous media;
- the role of axial diffusion due to turbulence in the overall mass transfer kinetics is negligible as compared to the film and solid phase diffusion;
- the model parameters such as distribution ratio K_d , liquid film coefficient β , solid phase diffusion coefficient D of substance as well as geometrical and hydrodynamic parameters of system under scope are independent from the concentration of substance and its placement in total system.

These assumptions mean the system is linear and a single dimensional (there is only one variable x —the bed length); time t should be used for description of system too. The models are formulated to satisfy exactly to a system of differential equations and boundary conditions.

2.1. Mass balance

Differential mass balance can be expressed as

$$v \frac{\partial c}{\partial x} + \varepsilon \frac{\partial c}{\partial t} + \frac{\partial a}{\partial t} = 0 \quad (1)$$

where c and a are the concentrations of solute in the mobile and in the stationary phases, v is the linear velocity of mobile phase and ε is the porosity of the column expressed as ratio of column void volume to the total volume of sorbent bed in the column. The concentrations are expressed in mass units of solute per unit of volume of mobile phase (c) or volume of stationary phase (a).

Table 1
The main characteristics of sorbents used for phenol preconcentration [13,19–21]

Sorbent	Manufacturer	Matrix nature	Cross-linking degree, %	Specific surface area S , $\text{m}^2 \text{g}^{-1}$	Pore diameter, Å	K_d (phenol), ml g^{-1}	Adsorption capacity of phenol, mg g^{-1}
KSK-G C ₁₆	BioChemMack	Silica-C ₁₆	–	250	–	1.7	1.2
Merrifield poly-styrene	Reanal	Ps-dvb ^a	2	–	–	3.2	0.4
Amberlite XAD-2	Serva	Ps-dvb ^a	8	300	90	79	0.7
Amberlite XAD-4	Serva	Ps-dvb ^a	16	750	50	270	1.1
PLRP-S 100	Polymer Labs	Ps-dvb ^a	60	500	100	–	2.1
Amberchrom CG-161	TosoHaas	Ps-dvb ^a	–	900	150	–	4.6
Envi-Chrom P	Supelco	Ps-dvb hcd ^b	100	800–950	110–175	–	4.2
LiChrolut EN	Merck	Ps-dvb hcd	100	1200	–	–	18
MN-100	Purolite Int.	Hcps ^c	> 100	1500	1000(15)	843	9.4
MN-150	Purolite Int.	Hcps	> 100	1070	300(14)	759	36
Purosorb MN-200	Purolite Int.	Hcps	> 100	1500	1000(11)	636	36

^a Ps-dvb—polystyrene-divinylbenzene.

^b Ps-dvb hcd—polystyrene-divinylbenzene with high cross-linking degree.

^c Hcps—hyper cross-linked polystyrene.

2.2. Mass transfer kinetics

Concerning liquid film diffusion model, the mass transfer rate can be expressed by the following equation:

$$\frac{\partial a}{\partial t} = \beta(c - f_{-1}(a)) \quad (2)$$

where β is the liquid film coefficient and $f_{-1}(a)$ is the reciprocal function of the adsorption isotherm of solute.

The solid phase diffusion model supposes the diffusion inside sorbent particles as the rate-limiting step. So, the mass transfer can be expressed as

$$\frac{\partial a^{(s)}}{\partial t} = \frac{1}{r^2} \frac{\partial}{\partial r} \left(r^2 D \frac{\partial a^{(s)}}{\partial r} \right) \quad (3)$$

where $a^{(s)}(x, t, r)$ is a local concentration of adsorbed substance inside of the sorbent particle; D is its apparent solid diffusion coefficient; r is the radius-vector from center of particle to its surface ($0 \leq r \leq \Re$, where \Re is the particle radius). The relation between the local concentration $a^{(s)}(x, t, r)$ of adsorbed substance and its average concentration over the volume of sorbent bed layer $a(x, t)$ is expressed by the following equation:

$$a(x, t) = \frac{3}{\Re^3} (1 - \varepsilon) \int_0^{\Re} a^{(s)}(x, t, r) r^2 dr \quad (4)$$

2.3. Equilibrium isotherm

The adsorption isotherm is assumed to be linear (Henry type):

$$a = \Gamma c, \quad (5)$$

where Γ is distribution ratio of the solute, calculated as ratio of its concentration in a volume of mobile phase to the concentration in a volume of stationary phase (ml ml^{-1}).

2.4. Initial and boundary conditions

Initial and boundary conditions are corresponded to the column operating under conventional preconcentration mode.

For liquid film diffusion:

$$c(x, 0) = 0_{x \neq 0}; \quad c(0, t) = \begin{cases} 0, & t = 0 \\ c_0, & t > 0 \end{cases};$$

$$a(x, 0) = 0 \quad (6)$$

and for solid phase diffusion:

$$c(x, 0) = 0_{x \neq 0}; \quad c(0, t) = \begin{cases} 0, & t = 0 \\ c_0, & t > 0 \end{cases};$$

$$a^{(s)}(x, 0, r) = 0; \quad a^{(s)}(x, t, \Re) = \frac{\Gamma c}{1 - \varepsilon};$$

$$\frac{\partial a^{(s)}(x, t, 0)}{\partial r} = 0$$

There is no solute both in liquid and solid phases at the beginning of the experiment.

2.5. Solutions

The introduction of dimensionless variables allows reducing the number of independent parameters in the system of equations Eqs. (1)–(5). Hence, the solution of system Eqs. (1)–(5) can be expressed by a number of dimensionless functions:

$$u(X, T) = c(x, t)/c_0; \quad q(X, T) = a(x, t)/\Gamma c_0;$$

$$q^{(s)}(X, T, \rho) = a^{(s)}(x, t, r)/(1 - \varepsilon)\Gamma c_0 \quad (8)$$

where $u(X, T)$, $q(X, T)$ and $q^{(s)}(X, T, \rho)$ are dimensionless concentrations of the solute, expressed per unit volume of mobile phase, stationary phase and sorbent particle, correspondingly; X, T and ρ is a set of dimensionless variables corresponding to length x , time t and radius-vector r in the particle: $X = x/\xi$, $T = t/\tau$, $\rho = r/\Re$. Parameters ξ and τ are the characteristic scales of length and time:

$$\xi = v/\beta, \quad \tau = \Gamma/\beta \quad (\text{liquid film diffusion model})$$

$$\xi = \Re^2 v/D\Gamma, \quad \tau = \Re^2/D \quad (\text{solid diffusion model}) \quad (9)$$

Solutions of system Eqs. (1)–(5) have been

obtained in a form suitable for numerical integration [27–29].

3. Experimental

The number of sorbents including hexadecylsilica KSK-G C₁₆ (BioChemMack, Moscow, Russia); Merrifield-type resin or chloromethylated poly(styrene-divinylbenzene) with 2% DVB (Reanal, Hungary); poly(styrene-divinylbenzene)s Amberchrom CG-161, XAD-2 and XAD-4 (all from Serva, Heidelberg, Germany); highly crosslinked poly(styrene-divinylbenzene)s Envi-Chrom P (Supelco, USA); hypercrosslinked polystyrenes Li-Chrolut EN (Merck, Germany), Purosorb MN-200, Macronet MN-100 and MN-150 series (all from Purolite Int, Pontyclun, UK) was studied in experiments on adsorption of phenol. The main characteristics of above listed sorbents are presented in Table 1.

The adsorption isotherms of phenol on hexadecylsilica, Amberlite XAD-2, XAD-4 resins, Purosorb MN-200, MN-150, MN-100 and Merrifield resin were obtained under static conditions by incubation of 0.02–0.5 g of sorbents with 5 ml of phenol solution (pH 2.0, 25 °C) during 24 h. Distribution ratios of phenol K_d (ml g⁻¹) and Γ (ml ml⁻¹) were calculated per unit of mass of sorbent and volume of stationary phase, correspondingly, from the transformed Langmuir equation ($a^{(s)} = Qkc/(1+kc)$, where Q is the maximum adsorption capacity, mg g⁻¹ and k is the Langmuir constant, ml mg⁻¹) as follows:

$$K_d = a^{(s)}/c; \quad \Gamma = (1 - \varepsilon)K_d \quad (10)$$

The concentration of phenol in solutions was determined by reversed-phase HPLC with photometric detection.

The kinetics of phenol adsorption was studied by the method of dynamic breakthrough curves [29]. Kinetic experiments under dynamic conditions were performed with isocratic liquid chromatograph consisted of high-pressure pump Beckman 114 M (Palo Alto, USA) and spectrophotometric detector microUVIS 20 (Carlo Erba Instr., Italy). The aqueous solution of phenol (pH 2.0, 25 °C) of constant concentration c_0 was

pumped through the column (70 mm × 2 mm i.d.) packed with sorbent at the constant flow rate of 0.5–3.0 ml min⁻¹. The concentration of phenol in effluent c was monitored photometrically at 280 nm, and time from the beginning of breakthrough experiment was registered for every sampling. The experiment was finished when c reached 98–99% of initial concentration c_0 . The incoming concentration of phenol c_0 was chosen as the highest value belonging to the linear part of adsorption isotherm to determine wide range of c values with maximum accuracy.

To determine the type of mass-transfer and calculate model's parameters, a simple but rather effective graphical solution of reciprocal task was used. The experimentally obtained breakthrough data plotted in bilogarithmic scale c/c_0-t were matched to the tabulated solution of system Eqs. (1)–(5) $u(X, T)$ build also in the same bilogarithmic scale as set of curves in coordinates $u-T$ [29]. As follows from Eqs. (8)–(10), the values of dimensional time t and its dimensionless equivalent T differ in bilogarithmic scale on a constant. Thus, the matching procedure consists in simple shift of breakthrough curve in parallel to time axis to find the best consistent calculated breakthrough curve. This matching yields a corresponding pairs of dimensional and dimensionless variables—sorbent bed length l and its equivalent X , time t and its equivalent T . The model's parameters such as liquid film coefficient β , apparent solid diffusion coefficient D , distribution ratio Γ (ml ml⁻¹) and K_d (ml g⁻¹) were calculated as follows from relations Eqs. (8)–(10):

$$\beta = X \frac{v}{l}; \quad \Gamma = \beta \frac{t}{T}$$

(liquid film diffusion model)

$$D = \Re^2 \frac{T}{t}; \quad \Gamma = X \frac{v \Re^2}{lD} \quad (\text{solid diffusion model})$$

$$K_d = \frac{\Gamma}{1 - \varepsilon} \quad (11)$$

The consistence among values of distribution ratio of phenol determined under batch condition

and calculated from breakthrough data was additionally used to prove the type of mass transfer.

When the good consistence among experimentally obtained breakthrough curve and tabulated solutions of system Eqs. (1)–(5) for both type of mass transfer was observed, the type of mass transfer was determined experimentally using stop-flow technique. In such cases the breakthrough experiment was repeated twice. In the second experiment, when the concentration of phenol in effluent reached 40–60% of its initial concentration, the solution flow was stopped inside a column for a time long enough to allow smoothing concentration gradients in sorbent particles (1–1.5 h). After that the breakthrough experiment was continued as described above. The breakthrough data obtained in both experiments were compared, excluding from calculation the period of time during which the solution flow was stopped. The coincidence of breakthrough curves proves the absence of significant contribution of diffusion in sorbent particles.

4. Results and discussion

The linear range of adsorption isotherm of phenol is the most crucial point in suitability of above-mentioned models and it has to be checked out before their application to calculations. The data on the adsorption of phenol on hexadecylsilica KSK-G C₁₆, Merrifield resin and hypercross-

linked polystyrenes of MN series were experimentally obtained and the literature data [30] were used for Amberlite XAD-2 and XAD-4 resins (Table 2). All isotherms have had a linear part (Henry's area) up to equilibrium concentration of phenol about 70 µg ml⁻¹. The distribution ratios of phenol K_d (ml g⁻¹) were calculated in linear concentration range in accordance with Langmuir equation (Table 1). Finally, incoming concentration 50 µg ml⁻¹ of phenol in water was chosen for the investigation of adsorption kinetics under dynamic conditions.

Experimental data on the adsorption of phenol on Merrifield resin and Amberlite XAD resins are corresponded to with the liquid film diffusion model (Fig. 1). In case of hexadecylsilica KSK-G C₁₆ and hypercrosslinked polystyrenes (MN-100, -150, -200) the definite choice between liquid film and solid diffusion models could not be done on the base of dynamic breakthrough curves only. The absence of reasonable impact of diffusion inside particles in overall mass transfer was proved in this case by stop-flow technique (Fig. 2). The calculated parameters of phenol adsorption according to film diffusion model are presented in Table 3.

Dynamic breakthrough curves of phenol on PLPR-S 100, Amberchrom CG-161, EnviChrom P and LiChrolut EN were accepted from [13]. These data are also in a good agreement with liquid film diffusion model (Fig. 3). The calculated model parameters for these sorbents are given in Table 3.

Distribution ratios of phenol K_d on hypercrosslinked polystyrenes MN determined in batch (Table 2) are in agreement with those calculated from breakthrough data (Table 3). This fact proves adequacy of the model chosen for the adsorption of phenol. The distribution ratios of phenol calculated from dynamic breakthrough curves for PLPR-S 100, Amberchrom CG-161, EnviChrom P, LiChrolut EN and Amberlite XAD are well correlated with their adsorption capacities determined in [13,19–21]. Some disagreement in K_d values published in literature (Table 1) and calculated from breakthrough data (Table 3) could be connected with non-linear conditions of dynamic adsorption systems used by the authors of

Table 2
Langmuir equation parameters ($n = 7$; $P = 0.95$)

Sorbent	Q , mg g ⁻¹	k , µl g ⁻¹	$K_d = Qk$, ml g ⁻¹
KSK-G C ₁₆	1.4 ± 0.1	1.57 ± 0.09	2.2 ± 0.3
Merrifield polystyrene	4.1 ± 0.5	1.27 ± 0.09	5.2 ± 0.8
Amberlite XAD-2	79 ± 4	1.65 ± 0.17	130 ± 7
Amberlite XAD-4	148 ± 6	1.69 ± 0.13	251 ± 7
MN-100	480 ± 60	1.9 ± 0.4	920 ± 100
MN-150	540 ± 40	1.6 ± 0.2	850 ± 50
Purosorb MN-200	202 ± 10	3.94 ± 0.35	795 ± 32

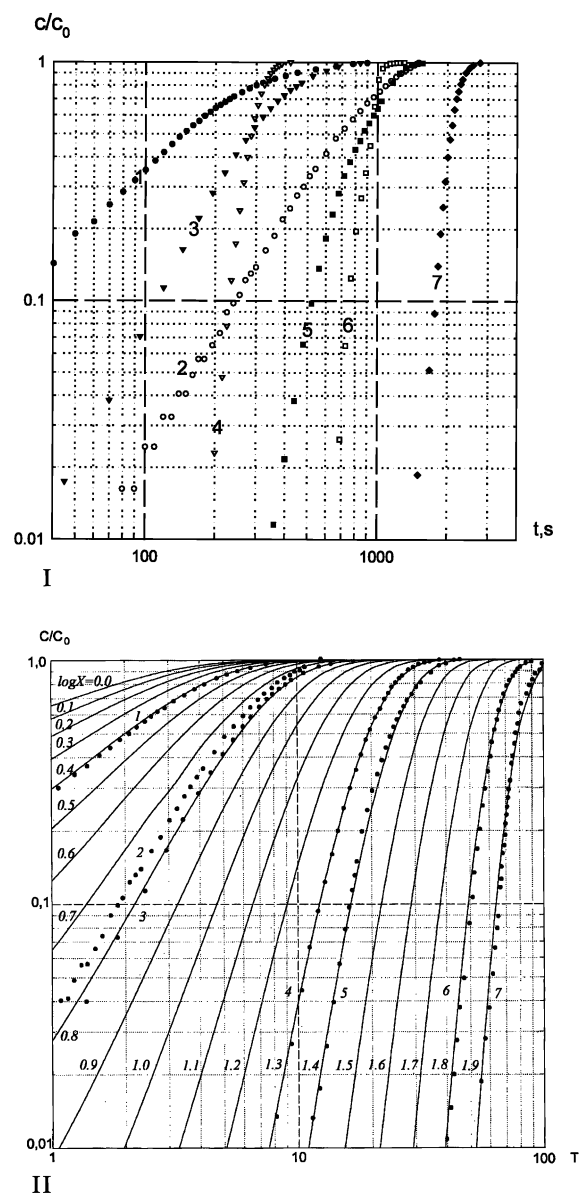


Fig. 1. Dynamic breakthrough curves of phenol on non-polar sorbents (experimental data). I—Experimental data: XAD-2 (1), XAD-4 (2), Merrifield-resin (3), hexadecylsilica KSK-G C₁₆ (4), MN-100 (5), Purosorb MN-200 (6), MN-150 (7); $v = 1.5$ (1), 0.7 (2–4); 3.0 (5), 2.5 (6), 2.0 (7) ml min⁻¹; weight of sorbent: 112 (1), 132 (2), 144 (3), 141 (4), 54.1 (5), 69.8 (6), 80.7 (7) mg; column 70 mm × 2 mm i.d. II—Calculated breakthrough curves (solid lines) for liquid film diffusion model matched to the experimental data.

[13,19–21]. Nevertheless, the calculated model parameters seem to be useful for evaluation of the adsorption efficiency of different adsorbents.

In opposite to sorption in batch mode, when the process efficiency is almost completely determined by distribution ratio K_d , neither this parameter, nor kinetic one (liquid film coefficient β , solid diffusion coefficient D) being considered separately can not be used as a measure of sorbent efficiency in column mode. Especially for sorption preconcentration in flow injection systems the term ‘concentration efficiency, CE’ was introduced by Fang [31] as ‘enhancement factor of analytical signal achieved per unit of time’. In our previous work [32], this term was applied to the sorption step only as the preconcentration factor K_{conc} achieved per unit of time under given value of recovery of solute R . Assuming nearly quantitative recovery of solute ($R \cong 1$) among assumptions stated above and calculating preconcentration factor per volume unit of sorbent bed:

$$CE = K_{\text{conc}}/t = a/c_0 t \cong w/V_{\text{bed}} = v/l \quad (12)$$

where w (ml min⁻¹) is flow rate and V_{bed} (ml) is a bed volume. According to this definition, the concentration efficiency is a measure of the column productivity in dynamic preconcentration of solute.

The peculiarity of mass transfer models described above is, that when model’s parameters (distribution ratio K_d and Γ , liquid film coefficient β , solid diffusion coefficient D , particle size \mathfrak{R}) are known and yet only preconcentration factor K_{conc} and recovery of solute R are given as limitative parameters, the maximum achievable in the system value of concentration efficiency CE_{max} could be calculated. On our opinion, this parameter being calculated for different systems under the same values of limitative parameters K_{conc} and R for could be considered as the total criterion of the sorbent efficiency. A method for evaluation of CE_{max} for liquid film and solid diffusion mass transfer is described below.

In dynamic preconcentration system with the conditions as stated above, at any time τ the preconcentration factor $K_{\text{conc}}(\tau)$ can be defined as:

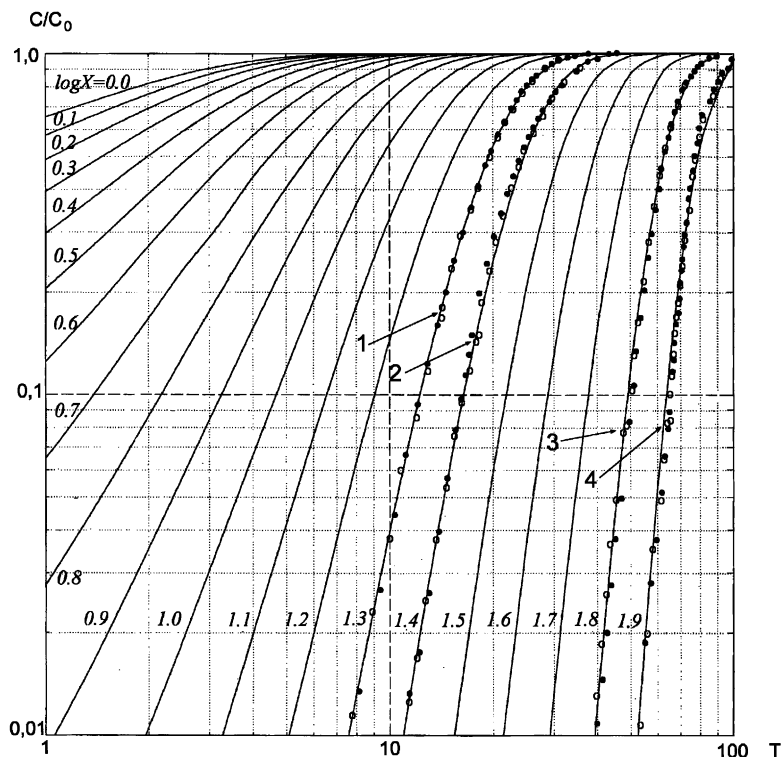


Fig. 2. Dynamic breakthrough curves of phenol obtained on non-polar sorbents in conventional mode (solid circles) and in stop-flow mode (hollow circles). Solid lines are calculated breakthrough curves for liquid film diffusion model matched to the experimental data. Sorbents and stop-flow time were: hexadecylsilica KSK-G C₁₆, 30 min (1); MN-100, 60 min (2); Purosorb MN-200, 60 min (3), MN-150, 60 min (4). Other experimental conditions are the same as on Fig. 1. Arrows mark the moments of stopping the flow.

$$K_{\text{conc}}(\tau) = \frac{1}{c_0 l} \int_0^l a(x, \tau) dx \quad (13)$$

As for infinite time ($\tau \rightarrow \infty$) $a(x, t) \rightarrow a_0$, the maximum preconcentration factor cannot be greater than Γ . Thus, in dynamic preconcentration

Table 3

The calculated parameters of liquid film diffusion model for the adsorption of phenol by non-polar sorbents

Sorbent	$R \times 10^{-3}$, cm	Γ , ml ml ⁻¹	K_d , ml g ⁻¹	β , s ⁻¹
KSK-G C ₁₆	7.1	30.1 ± 1.9	47 ± 3	1.06 ± 0.05
Merrifield polystyrene	3.0	20.5 ± 1.3	31 ± 2	0.37 ± 0.02
Amberlite XAD-2	18.9	24.4 ± 2.1	46 ± 4	0.39 ± 0.02
Amberlite XAD-4	23.9	39.6 ± 0.6	66 ± 1	0.31 ± 0.01
PLPR-S 100 ^a	1.0	129 ± 6	430 ± 20	19.4 ± 0.5
Amberchrom CG-161 ^a	3.8	249 ± 21	1080 ± 90	4.7 ± 0.5
Envi-Chrom P ^a	6.0	242 ± 16	1050 ± 70	3.6 ± 0.2
LiChrolut EN ^a	4.0	575 ± 37	2500 ± 160	7.3 ± 0.5
MN-100	3.0	197 ± 2	800 ± 10	5.5 ± 0.3
MN-150	3.0	326 ± 4	880 ± 10	13.6 ± 0.8
Purosorb MN-200	5.0	250 ± 7	780 ± 20	15.5 ± 0.2

^a Calculated on the literature data [13].

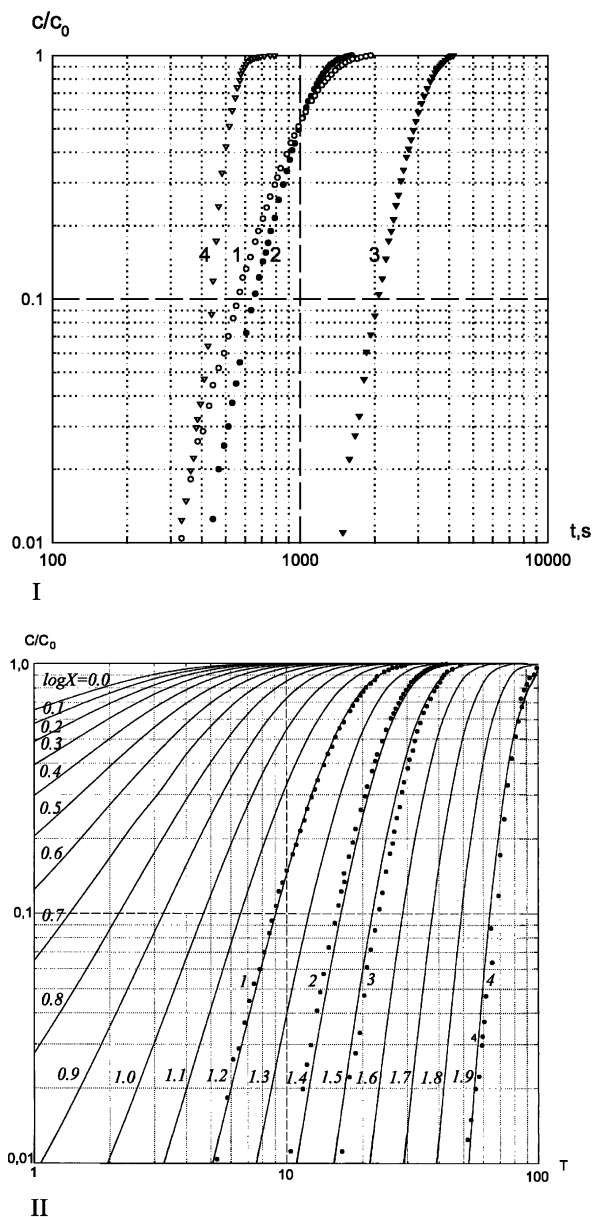


Fig. 3. Dynamic breakthrough curves of phenol on non-polar sorbents (according to [13]). I—Experimental data: Envi-Chrom P (1), Amberchrom CG-161 (2), LiChrolut EN (3), PLPR-S 100 (4); $v = 1.0 \text{ ml min}^{-1}$; sorbent mass: 16.3 (1–3), 21.2 (4) mg; column: 10 mm \times 3 mm i.d. II—Calculated breakthrough curves (solid lines) for liquid film diffusion model matched to the experimental data.

system the preconcentration factor per unit of its maximum value Γ (in fact, the ‘expanded capacity of sorbent bed’) can be expressed as:

$$\frac{K_{\text{conc}}(\tau)}{\Gamma} = \frac{1}{a_0 l} \int_0^l a(x, \tau) dx \quad (14)$$

At the same time the recovery of solute $R(\tau)$ can be written as:

$$\begin{aligned} R(\tau) &= \frac{c_0 w \tau - w \int_0^\tau c(l, t) dt}{c_0 w \tau} \\ &= 1 - \frac{1}{c_0 \tau} \int_0^\tau c(l, t) dt \end{aligned} \quad (15)$$

This gives us the ‘cumulative breakthrough’:

$$1 - R(\tau) = \frac{1}{c_0 \tau} \int_0^\tau c(l, t) dt \quad (16)$$

As regards to solution of the system Eqs. (1)–(5) in dimensionless form, the expanded capacity of sorbent bed and the cumulative breakthrough can be written in the following form:

$$\eta(X, T) = \frac{K_{\text{conc}}}{\Gamma} = \frac{1}{X} \int_0^X q(X, T) dX \quad (17)$$

$$\chi(X, T) = 1 - R = \frac{1}{T} \int_0^T u(X, T) dT \quad (18)$$

These functions were calculated according to relations Eqs. (17) and (18) from tabulated solutions of the system Eqs. (1)–(5) by numerical integration [29].

Graphical solution of the system Eqs. (17) and (18) for liquid film diffusion mass transfer is demonstrated on Fig. 4. Calculated functions $\eta(X, T)$ and $\chi(X, T)$ were plotted as a set of curves in coordinate plane X – T . The cross point of two curves for given values of η (distribution ratio Γ and preconcentration factor K_{conc}) and χ (recovery R) gives the values of dimensionless parameters X_{max} and T_{max} . The concentration efficiency CE_{max} and corresponding dimensional

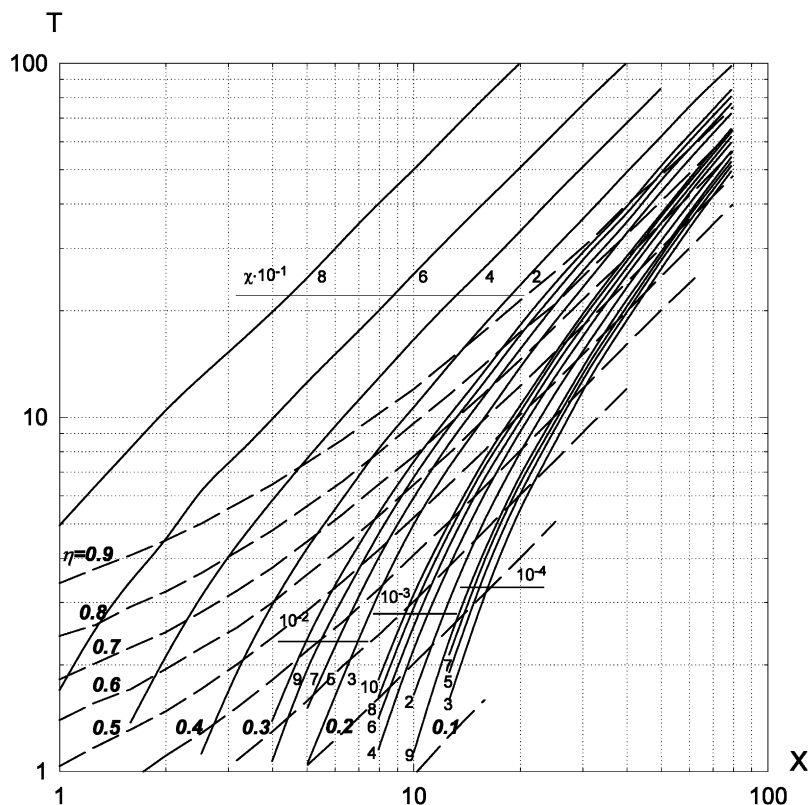


Fig. 4. Graphical evaluation of the maximum achievable preconcentration efficiency CE_{\max} for liquid film diffusion model. The cross point of curves representing the calculated parameters η (dashed lines) and χ (solid lines) gives the values of dimensionless bed length X_{\max} and time T_{\max} for given preconcentration factor K_{conc} , distribution ratio (K_d , Γ) and recovery of solute R .

sorption time t_{\max} are calculated from relations Eq. (9):

$$CE_{\max} = \frac{\beta}{X_{\max}}; \quad t_{\max} = \frac{T_{\max} \Gamma}{\beta} \quad (19)$$

(liquid diffusion model)

$$CE_{\max} = \frac{D \Gamma}{X_{\max} \Re^2}; \quad t_{\max} = \frac{T_{\max} \Re^2}{D} \quad (20)$$

(solid diffusion model)

It should be noted that this method allows the extremely useful tool for comparison of efficiency for various dynamic adsorption systems under different but optimum in each case conditions. If calculated CE_{\max} could not be achieved on some reasons (for instance on poor hydrodynamics), this parameter can still be useful for characterization of system stability. This stability allows perform-

ing successful preconcentration of solute from solutions of complex composition, where the distribution ratio of solute could be much lower than in model solutions.

To compare the efficiency of sorbents under scope of present work for preconcentration of phenol, the values of CE_{\max} and corresponding sorption time t_{\max} were calculated according to proposed method. The values of preconcentration factors K_{conc} of 10 and 100 and the recovery of phenol $R = 95\%$ were chosen as limitative parameters. The corresponding values of η and χ were obtained for each system from relations Eqs. (10), (17) and (18) using determined distribution ratios of phenol and information about bed density. Then dimensionless parameters X_{\max} and T_{\max} were calculated by numerical solution of the system Eqs. (17) and (18) and finally, the values

of CE_{\max} and t_{\max} were obtained from Eq. (19). For some sorbents and preconcentration factor 10 the values X_{\max} and T_{\max} were outside of bounds used in calculations. In such a case the solution of system Eqs. (17) and (18) and the values of CE_{\max} and t_{\max} were estimated by graphical extrapolation. The results are summarized in Table 4.

The application of models Eqs. (1)–(5) allows determining the impact of both kinetic and thermodynamic factors in total concentration efficiency. As the liquid film diffusion mass transfer is proved, the model parameters are the liquid film coefficient β and the distribution ratio K_d . The value of β includes impacts of convection, molecular and longitudinal diffusion which dependent from the properties of liquid and solid phases, i.e. by the diffusion rate of the solute in solution, the apparent surface of liquid–solid boundary etc, and by the hydrodynamic type of the flow of mobile phase.

Distribution ratio K_d reflects the sorption thermodynamics. The results obtained show that the distribution ratios of phenol for highly and hypercrosslinked polystyreness (cross-linking degree is more than 100%) are considerably higher than for hexadecylsilica and poly(styrene-divinylbenzene)s with low cross-linking degree (2–16%). An intermediate K_d was observed for PLRP-S 100

having cross-linking degree equal to 60%. Consequently, the change in cross-linking degree results in change of sorbate–sorbent interaction energy for polymer sorbents.

According to [33], the mechanism of adsorption of organic molecules on polymeric sorbents includes either adsorption on the surface or dissolving in a solid phase, or mixed mode. It should be noted that the relative impact of each process depends on the microstructure of polymer. An increase of cross-linking degree seems to result in slow change of retention mechanism from preferable adsorption to distribution. It leads to remarkable increase in adsorption capacity as well as in distribution ratio [34,35].

An role of porous structure of poly(styrene-divinylbenzene)s and carbon black in retention of some test compounds was studied in [36,37]. According to these data, the retention of hydrocarbons, alcohols and esters on polymeric sorbent with cross-linking degree 43% ($S = 590 \text{ m}^2 \text{ g}^{-1}$) is approximately in 3 times stronger than on sorbent with cross-linking degree 25% ($S = 183 \text{ m}^2 \text{ g}^{-1}$). Also, the increase in surface area of carbon black from 15 to $150 \text{ m}^2 \text{ g}^{-1}$ results in 10 times increase of retention. Obviously, the retention is proportional to the value of specific surface area of sorbents. In case of hypercrosslinked polystyrenes

Table 4

Calculated maximum achievable concentration efficiency CE_{\max} and corresponding preconcentration time t_{\max} for the phenol recovery on reversed-phase sorbents

Sorbent	$K_{\text{conc}} = 10$		$K_{\text{conc}} = 100$	
	$CE_{\max}, \text{min}^{-1}$	t_{\max}, min	$CE_{\max}, \text{min}^{-1}$	t_{\max}, min
KSK-G C16	11.0	0.97	— ^a	— ^a
Merrifield polystyrene	2.7	4.0	— ^a	— ^a
Amberlite XAD-2	3.4	3.0	— ^a	— ^a
Amberlite XAD-4	3.9	2.8	— ^a	— ^a
PLPR-S 100 ^b	> 300	< 0.04	44	2.4
Amberchrom CG-161 ^b	> 110	< 0.09	43	2.5
Envi-Chrom P ^b	> 90	< 0.1	32	3.2
LiChrolut EN 8 ^b	> 180	< 0.08	110	1.05
MN-100 ^b	> 130	< 0.08	38	2.8
MN-150 ^b	> 300	< 0.04	155	0.68
Purosorb MN-200 ^b	> 300	< 0.04	140	0.75

The recovery of phenol 95%, preconcentration factors 10 and 100.

^a Preconcentration factor 100 could not be achieved.

^b Values of CE_{\max} and t_{\max} for $K_{\text{conc}} = 10$ were estimated by graphical extrapolation.

($S = 1500 \text{ m}^2 \text{ g}^{-1}$) the retention of organic molecules increased drastically (in 6–7 times) as well as adsorption capacities for these polymers. Therefore, the increase of cross-linking degree leads to the change of retention mechanism.

Poly(styrene-divinylbenzene) sorbents are found the most efficient substrates for the preconcentration of phenol from water solution by SPE. The advantage of this group of sorbents is expressed sharply for polymers with high cross-linking degree (60% and more). The difference between values of CE_{max} calculated for hypercrosslinked polystyrene and Merrifield resin of gel type is about two orders of magnitude. Preconcentration factor of 100 can not be achieved with hexadecyl-silica or with poly(styrene-divinylbenzene) resins of low cross-linking degree.

5. Conclusions

The method based on LMSD allows to compare phenol preconcentration efficiency of different sorbents under dynamic conditions. This approach may be useful for the optimal choice of sorbent in water purification and in analytical chemistry for preconcentration of trace organic compounds by SPE. The highly crosslinked poly(styrene-divinylbenzene) and hypercrosslinked polystyrene were found the most promising for phenol preconcentration.

Acknowledgements

The authors thanks to Prof E.V. Venitsianov for the helpful discussion on LMSD.

References

- [1] J.C. Hoffsommer, D.J. Glover, C.Y. Hazzard, J. Chromatogr. 195 (1980) 435.
- [2] G. Marko-Varga, D. Barselo, Chromatographia 34 (1992) 146.
- [3] D. Puig, D. Barselo, J. Chromatogr. A 778 (1997) 313.
- [4] (a) V.V. Goncharov, V.B. Goryunova, V.M. Tul'chinskii, Zavodsk. Laboratoriya 58 (1) (1992) 10;
- (b) V.V. Goncharov, V.B. Goryunova, V.M. Tul'chinskii, Zavodsk. Ind. Lab. 58 (1) (1992) 15.
- [5] (a) Ya.I. Korenman, R.P. Lisitskaya, Zavodsk. Laboratoriya (Diag. Mater.) 64 (6) (1998) 3;
- (b) Ya.I. Korenman, R.P. Lisitskaya, Ind. Lab. (Diag. Mater.) 64 (3) (1998) 3.
- [6] V. Piangerelli, F. Nerini, S. Cavalli, Annali di Chimica 83 (1993) 331.
- [7] C.W. Klampfl, E. Spanos, J. Chromatogr. A 715 (1995) 213.
- [8] M. Castillo, D. Puig, D. Barselo, J. Chromatogr. A 778 (1997) 301.
- [9] (a) I.Yu. Andreeva, L.L. Kuvaldina, Zh. Anal. Khim. 50 (1995) 45;
- (b) I.Yu. Andreeva, L.L. Kuvaldina, J. Anal. Chem. 50 (1995) 42.
- [10] N. Masque, R.M. Marce, F. Borrull, J. Chromatogr. A 793 (1998) 257.
- [11] N.A. Penner, P.N. Nesterenko, A.V. Khryashevsky, T.N. Stranadko, O.A. Shpigun, Mendeleev Commun. 1 (1998) 24.
- [12] P. Musmann, K. Levsen, W. Radeck, Fresen. J. Anal. Chem. 348 (1994) 654.
- [13] N. Masque, R.M. Marce, F. Borrull, Trends in Anal. Chem. 17 (1998) 384.
- [14] F. Mijangos, A. Navarro, J. Chem. Eng. Data 40 (1995) 875.
- [15] M.-W. Jung, D.W. Lee, J.-S. Rhee, K.-J. Paeng, Anal. Sci. 12 (1996) 981.
- [16] B. Gawdzik, J. Gawdzik, U. Czerwinska-Bil, J. Chromatogr. 509 (1990) 135.
- [17] D.C. Kennedy, Ind. Eng. Chem. Prod. Res. Develop. 12 (1973) 56.
- [18] E.H. Crook, R.P. McDonnel, J.T. McNulty, Ind. Eng. Chem. Prod. Res. Develop. 14 (1975) 113.
- [19] N. Masque, M. Galia, R.M. Marce, F. Borrull, J. Chromatogr. A 771 (1997) 55.
- [20] PLRP-S 100A. Polymeric Reversed Phase HPLC Columns and Media. Polymer Laboratories.
- [21] O. Fiehn, M. Jekel, Anal. Chem. 68 (1996) 3083.
- [22] N.A. Penner, P.N. Nesterenko, M.M. Ilyin, M.P. Tsyurupa, V.A. Davankov, Chromatographia 50 (1999) 611.
- [23] M.P. Tsyurupa, L.A. Maslova, A.I. Andreeva, T.A. Mrachkovskaya, V.A. Davankov, React. Polym. 25 (1995) 69.
- [24] Hypersol-MacronetTM, Sorbent Resins, Purolite Technical Bulletin, The Purolite Company, 1995.
- [25] A.V. Khryashevskii, M.V. Podlovchenko, P.N. Nesterenko, O.A. Shpigun, Moscow Univ. Chem. Bull. 39 (3) (1998) 196.
- [26] V. Coquart, M.-C. Hennion, J. Chromatogr. A 600 (1992) 195.
- [27] A. Anzelius, Z. Angew. Math. Mech. 6 (1926) 291.
- [28] J.B. Rosen, J. Chem. Phys. 20 (3) (1952) 387.
- [29] E.V. Venitsianov, R.N. Rubinshtein, Dinamika sorbcii iz zhidkih sred (Dynamics of Sorption from Liquid Media), Nauka, Moscow, 1983.

- [30] F. Mijangos, A. Navarro, *J. Chem. Eng. Data* 40 (1995) 875.
- [31] Zh. Fang, *Flow Injection Atomic Absorption Spectrometry*, Wiley, New York, 1995.
- [32] E.V. Venitsianov, I.A. Kovalev, G.I. Tsylin, *Teoriya i praktika sorbcionnyh processov* (Theory and Practice of Sorption Processes), vol. 23, Voronezh, 1998, p. 24.
- [33] A.V. Kiselev, Ya.I. Yashin, *Gas-Adsorption Chromatography*, Plenum Press, New York, 1969.
- [34] B. Versino, F. Geiss, *Chromatographia* 2 (1969) 354.
- [35] J.F. Johnson, E.M. Barrall, *J. Chromatogr.* 31 (1967) 547.
- [36] (a) L.D. Belyakova, A.M. Voloschuk, L.M. Vorobjeva, O.A. Larionova, O.G. Larionov, *Zh. Phys. Khimii.* 69 (1995) 501;
(b) L.D. Belyakova, A.M. Voloschuk, L.M. Vorobjeva, O.A. Larionova, O.G. Larionov, *J. Phys. Chem.* 69 (1995) 455.
- [37] (a) L.D. Belyakova, O.V. Vasilevskaya, M.P. Tsyurupa, V.A. Davankov, *Zh. Phys. Khimii.* 70 (1996) 1476;
(b) L.D. Belyakova, O.V. Vasilevskaya, M.P. Tsyurupa, V.A. Davankov, *J. Phys. Chem.* 70 (1996) 1374.